Torres-Giner, S.; Torres, A.; Ferrándiz, M.; Fombuena, V.; Balart, R. (2017). Antimicrobial activity of metal cation-exchanged zeolites and their evaluation on injection-molded pieces of bio-based high-density polyethylene. Journal of Food Safety. 37(4). doi:10.1111/jfs.12348

Antimicrobial evaluation of injection-molded pieces of bio-based high-density polyethylene containing metal cation-exchanged zeolites of interest in food hygiene

Sergio Torres-Giner[1*], Ana Torres[2], Marcela Ferrándiz[2], Vicent Fombuena[1], and Rafael Balart[1]

[1]*Technological Institute of Materials (ITM), Universitat Politècnica de València (UPV), Plaza Ferrándiz y Carbonell 1, 03801 Alcoy, Spain*

[2]*Textile Industry Research Association (AITEX), Plaza Emilio Sala 1, 03801 Alcoy, Spain*

[*]*Corresponding author: Dr. Sergio Torres-Giner. Email: storresginer@hotmail.com*

ABSTRACT. In this study three different natural types of zeolite (chabazite, mordenite, and faujasite) were characterized for their morphology, elemental composition, and antimicrobial activity against food-borne bacteria and fungi. Morphological and chemical characterization of zeolites was carried out using Scanning Electron Microscopy (SEM) and X-Ray Fluorescence (XRF), respectively. Their antimicrobial activity was evaluated against *Staphylococcus aureus (S. aureus)*, *Escherichia coli (E. coli)*, *Pseudomonas aeruginosa (P. aeruginosa)*, *Aspergilus niger* (*A. niger*), and *Candida albicans* (*C. albicans*). The chabazite–type zeolite was selected due to its improved morphology and lowest ratio of silica/alumina (Si/Al). This was then solution exchanged with silver (Ag^{+}), copper (Cu^{2+}), and zinc (Zn^{2+}) ions to prepare single, binary, and ternary metal cation-modified zeolites. Obtained results indicated that the multi-ionic ternary system, *i.e.*, the Ag-Cu-Zn-zeolite, was the most promising antimicrobial material. In a last step, this was for the first time incorporated into a bio-based, *i.e.*, derived of sugar cane, high-density polyethylene (bio-HDPE) by extrusion followed by injection molding. Sustainable polymer composite pieces with balanced mechanical properties and high biocide performance were obtained. These offer industrial relevance in hygiene applications to control the growth of harmful microorganisms in food contact materials such as plastic handles, cutlery, rigid packaging, kitchen furnishing, cutting boards, and decontamination surfaces.

Keyword: Bio-based polyethylene, Metal cation-exchanged zeolites, Injection molding, Antimicrobial properties, Food hygiene.

1. Introduction.

Control of microbial growth in the packaging environment is a key parameter to avoid food waste (Torres-Giner et al., 2014). A high hygienic status of surfaces that come in contact with food is also important to reduce the risk of cross-contamination of unwanted microorganisms (Reij et al., 2004). The growth of spoilage microorganisms cannot only reduce food shelf life, but the spread of pathogenic microorganisms endangers public health. Materials containing antimicrobials, also referred as "treated" materials, have been recently introduced to the food sector as a new concept to improve hygiene (Møretrø and Langsrud, 2011). Active-releasing antimicrobial systems can be generated by different ways such as through coatings or compounds absorbed on the material surfaces, volatile and non-volatile substances directly incorporated into the plastic parts, immobilization onto polymer matrices by ion or covalent linkages, and materials that are inherently antimicrobial (Appendini and Hotchkiss, 2002). For achieving long-term protection functionality against harmful microorganisms, a sustained release profile of the biocide is habitually preferred (Torres-Giner, 2011).

Zeolites are three-dimensional (3D) microporous crystalline solids composed of silicon (Si^{4+}) and aluminum (Al^{3+}) that are tetrahedrally coordinated with each other by corner-sharing oxygen atoms (SiO_4^{4-} and AlO_4^{5-}) (Suib, 2003). Isomorphic substitution of Al^{3+} by Si^{4+} leads to a negatively charged aluminosilicate framework in the form of channels or interconnected voids. This can be naturally counter-balanced by alkaline or alkaline-earth metal cations such as sodium (Na^+) and potassium (K^+), which are coordinated with a well-defined number of water molecules. These can be readily exchanged in solution by other cations such as heavy metals and ammonium ions (Rozic et al., 2000). The cation exchange capability of zeolites highly depends on their ratio of silica/alumina (Si/Al), which increases as this ratio decreases (Saint-Cricq et al., 2012). According to this, there are several types of natural and synthetic zeolites with high porosity features that can accommodate active molecules inside their interconnected cavities (Corma and Garcia, 2004). This has recently

54 placed zeolites in the focus of study as cargo carriers for the sustained release of biocides in
55 food contact applications (Duncan, 2011).

56 Heavy metals have been long recognized for their broad-spectrum bacteriostatic and
57 bactericidal activity. Among them, silver (Ag) presents the largest antimicrobial capacity. At
58 present, zeolites have been extensively considered as a promising inorganic reservoir for
59 hosting silver ions (Ag^{+}) with a controlled release capacity (Egger et al., 2009; Ferreira et al.,
60 2012; Inoue and Hamashima, 2012; Kwakye-Awuah et al., 2008; Saint-Cricq et al., 2012).
61 Silver-loaded antibacterial zeolite (Ag–zeolite) is habitually prepared by ion exchange
62 solutions based on silver nitrate ($AgNO_3$) in which the resultant silver content in zeolites is
63 typically in the range of 50–60 mg/g (Krishnani et al., 2012; Lalueza et al., 2012). Other
64 metals such as cobalt (Co), nickel (Ni), copper (Cu), zinc (Zn), zirconium (Zr), molybdenum
65 (Mo), and lead (Pb) have also showed to exhibit antibacterial properties against both Gram-
66 positive and Gram-negative bacterial strains (Yasuyuki et al., 2010). Some of these metals
67 have been already loaded into clinoptilolite-rich natural zeolite to investigate the antibacterial
68 activity of the resultant materials (Top and Ulku, 2004). The metal-loading process is actually
69 a cation exchange process on the zeolite structure between sodium ions (Na^{+}) with Ag^{+} as
70 well as other metal cations such as copper (Cu^{+2}) and zinc (Zn^{+2}) ions. During this process the
71 electrostatic charge of the zeolite lattice polarizes metal ions to form dipoles, directing their
72 positively charged end to the lattice (Czaran et al., 1989).

73 Metal cation-modified zeolites can be potentially employed as antimicrobial fillers into
74 polymer matrices. These novel polymer composites can attract some commercial and
75 industrial interest, mainly for biomedical and food packaging applications. However, so far
76 only a few studies have been focused on the biocide activity of polymer materials containing
77 such functionalized zeolites. These mainly include polypropylene (PP) (Li et al., 2013;
78 Pehlivan et al., 2005), thermoplastic polyurethane (TPU) (Kaali et al., 2011; Kamisoglu et al.,
79 2008), polylactic acid (PLA) (Fernandez et al., 2010), polyvinyl chloride (PVC) (Zampino et
80 al., 2011), low-density polyethylene (LDPE) (Boschetto et al., 2012), ethylene vinyl acetate
81 (EVA) (Mishra et al., 2013), and poly (vinyl alcohol) (PVA) (Narin et al., 2014).

Incorporation of antimicrobial zeolites into polymer matrices by melt compounding makes it more advantageous and applicable than conventional approaches (*e.g.*, direct material deposition). This can be explained because metal ions are more effective than metallic atoms (Kamisoglu et al., 2008). Also, the antimicrobial activity can be prolonged since the release rate out of the polymer composite is mainly determined by the diffusion of ions from top material layers (Boschetto et al., 2012). Finally, the antimicrobial material uses can be further increased as both sides of the plastic part becomes antimicrobial (Zampino et al., 2011).

Linking of silver to zeolite, as the carrier support, represents a cost-effective alternative than the direct use of silver compounds in food applications (*e.g.*, $AgNO_3$ solution and silver plate) (Matsumura et al., 2003). However, there is a growing concern about the potential toxicity related to Ag^+ migration into food (Yang et al., 2009). Whereas relatively high concentrations of silver ions, *i.e.*, over 5 mg Ag^+/kg, are habitually necessary to achieve antimicrobial performance (Del Nobile et al., 2004), these are probably unacceptable at the view of the current legislation that regulates the presence of silver in food (Rai et al., 2009). For this reason, Ag-zeolites have been recently proposed for hygiene applications such as antifouling coatings on stainless steel (Griffith et al., 2015), drinking water treatment (Gehrke et al., 2015), and cutting boards (Møretrø et al., 2012).

Bio-based polyethylene, also called “microbial” or “green” polyethylene, is produced by catalytic dehydration of bioethanol followed by conventional polyethylene polymerization (Chen et al., 2007). Bioethanol is obtained by microbial strain and/or biological fermentation from renewable feedstock, including sugar cane and beet or starch crops (*e.g.*, maize, wheat, wood, and other plant wastes). Bio-based polyethylene has exactly the same chemical and physical properties as its petrochemical counterpart polymer (Babu et al., 2013). In particular, bio-based high-density polyethylene (bio-HDPE) is an excellent sustainable rigid material that could be targeted towards hygiene uses. These include different materials in contact with food such as cutting boards, kitchen utensils and countertops, and storage containers.

Herein, the preparation and characterization of bio-HDPE composites containing antimicrobial zeolites by injection molding was first reported. For this, the optimal type of

zeolite was first examined. The selected zeolite was then metal cation-modified with Ag^{+}, Cu^{+2}, Zn^{+2} through an ion exchange solution process. The antimicrobial activities against food-borne bacteria and fungi were monitored. Furthermore, as a key requirement for rigid applications, mechanical tests were performed in order to ascertain the suitability of this novel sustainable polymer composite.

2. Experimental

2.1. Materials

Commercial zeolite Sapo-34 (CFT-03) with a chabazite topology was supplied by Tianjin Chemist Scientific, Ltd. (Tianjin, China). Mordenite CBV-10A and faujasite (Y-type) CBV-100 were both provided by Zeolyst International (Valley Forge, USA). $AgNO_3$, copper nitrate ($Cu(NO_3)_2$), and zinc nitrate ($Zn(NO_3)_2$) were obtained from Sigma Aldrich (Madrid, Spain).

Commercial green HDPE SHA 7260 with a melt flow index (MFI) of 20 g/10 min and a density of 0.955 g/cm^3 was provided by FKuR Kunststoff GmbH (Willich, Germany). This bio-HDPE is produced from ethanol derived from sugar cane with a minimum natural content of 94.5% according to manufacturer Braskem (Sao Paulo, Brasil). The resin is specifically designed for injection molding and fiber extrusion.

2.2. Metal cation exchange

The selected zeolite was chemically modified using different combinations of metal cations (Ag^{+}, Cu^{+2}, and Zn^{+2}) as summarized in **Table 1**. Following aqueous solutions were prepared for the ion exchange process: 0.07 M $AgNO_3$, 0.2 M $Zn(NO_3)_2 \cdot 6H_2O$, and 0.4 M $Cu(NO_3)_2 \cdot 3H_2O$. The process was carried out by magnetically stirring 50 g of zeolite powder at 500 rpm during 30 min with 100 mL of distilled water at 40 ºC. Once the first homogenization process was accomplished, 150 mL of the different cation solutions were added for additional 24 h to allow ion interchange. To complete the process, the resultant solution was washed five times with distilled water, filtered, and the residual powder dried in

oven at 90 ºC for 1 h. **Figure 1** shows the scheme of the metal cation-exchange process carried out on zeolite.

2.3. Preparation of polymer composites

The selected metal-cation exchanged zeolites were incorporated in powder form at different weight amounts (1, 5, 10, and 15 wt.-%) into bio-HDPE. The materials were melt-compounded at 170 ºC and 40 rpm in a twin-screw co-rotating extruder D30 model from Dupra (Alicante, Spain). Composites were extruded through a round die to produce strands, which solidified by passing through a water bath and were then pelletized. Resultant polymer composite pellets were shaped in an injection machine Meteor 270/75 from Mateu and Solé (Barcelona, Spain) at 190 ºC using a mirror-finishing steel mold with standard geometries for sample characterization. A clamping force of 75 tons was applied.

2.4. Material characterization

Elemental composition of the as received zeolites and metal cation-modified zeolites was determined by X-ray fluorescence (XRF) using a Magix Pro PW2400 from Philips Analytical (Almelo, The Netherlands). This system was equipped with a beryllium screen and samples were analyzed in powder form by a rhodium target excited at 30 kV and 150 mA. Analyses were done by duplicate under a helium atmosphere.

Morphology of the zeolite samples was observed by Scanning Electron Microscoscopy (SEM) using a JSM-6300 from JEOL Ltd. (Tokyo, Japan) at an emissive mode of 20 kV. Zeolite powder was deposited on a double-sided carbon conductive scotch tape. Samples were examined on the surface after being coated with a fine layer of gold–palladium alloy under vacuum conditions in a Sputter Coater EMITECH model SC7620 from Quorum Technologies Ltd (East Sussex, UK).

Elastic modulus (E), elongation at break (σ), and tensile strength (ε) of the injection-molded composite pieces were measured using a universal test machine Elib 30 from Ibertest S.A.E. (Madrid, Spain) according to ISO 527. Six samples were tested and the values were

166 averaged. Shore D hardness values were attained in a hardness durometer model 676-D from
167 J. Bot Instruments (Barcelona, Spain) following the guidelines of ISO 868.
168
169 ***2.5. Antimicrobial Properties***
170 Antibacterial properties were determined for bacterial cultures from American Type
171 Culture Collection (ATCC) of *Staphylococcus aureus* (*S. aureus*) ATCC 6538, *Escherichia*
172 *coli* (*E. coli*) ATCC 25922, and *Pseudomonas aeruginosa* (*P. aeruginosa*) ATCC 9027. Tests
173 followed guidelines of ASTM E 2149-10 and cultures were cultivated in tryptone soy broth
174 (TSB) from Oxoid Thermo Scientific (Basingstoke, UK). These were then spread on a plate
175 count Agar at 35 ± 2 ºC for 24 h. Colony forming units per milliliter (CFU/mL) were
176 accurately and reproducibly obtained. Antifungal activity was tested against *Aspergilus niger*
177 (*A. niger*) ATCC 6275 and *Candida albicans* (*C. albicans*) ATCC 10231. The ATCC test 30-
178 2004 (Method III) was used, for this an incubation temperature of 28 ± 2 ºC was selected. The
179 microorganisms growth range was quantified as follows: 0 as no growth, 1 as growth only
180 visible by microscopy, 2 as macroscopic growth (traces lower than 10%), 3 as small growth
181 (traces between 10 and 30%), 4 as medium growth (traces between 30 and 60%), and 5 as
182 high growth (traces higher than 60%).
183 Biocide performance of the injection-molded composite pieces was evaluated for the
184 same bacteria. This was done according to the Japanese industrial standard (JIS) Z 2801:2013
185 with a contact time of 24 h. This is a common method for assessing the antimicrobial activity
186 of materials in hygiene applications (Møretrø and Langsrud, 2011). Bacteria were deposited
187 in suspension on the test surface. The antibacterial activity was taken as the test surface
188 reduction (R) using the expression:
189
190 $$R = \log\frac{B}{C} \qquad (1)$$
191

Where B is the CFU/mL of the control sample and C is the UFC/mL of the reference sample, both measured after 24 h. A given sample presents antibacterial activity if $R \geq 2$.

3. Results and discussion

3.1. Selection of the unmodified zeolite

Zeolite crystals with different morphologies can be observed in the SEM micrographs shown in **Figure 2**. **Figure 2a** indicates that the unmodified chabazite-type zeolite crystallized in a triclinic crystal system to form rhombohedral-shaped crystals. These presented concise dimensions between 5 and 25 μm with a bimodal particle size distribution. A similar cube-like morphology was recently observed for unmodified zeolite particles (Li et al., 2013). It has been previously reported that an uniform morphology is optimal for chemical cation exchange and for achieving homogenous distribution in a polymer matrix (Lopes et al., 2013). While the surface of chabazite was relatively smooth, mordenite (**Figure 1b**) and faujasite (**Figure 1c**) did not display a definite crystal shape. At higher magnifications, the morphology of mordenite still remained undefined. However, closer observations revealed that faujasite particles presented a round-like morphology with a rough surface. Zeolite crystal sizes were in the range of 3–8 μm and 1–6 μm, for mordenite and faujasite samples, respectively. In both cases, coarse particles or aggregates higher than 50 μm were observed. Recently, faujasite was described to crystallize in an octahedral shape of *ca.* 9 μm (Demirci et al., 2014).

Table 2 shows the chemical composition of the unmodified zeolites obtained by XRF analysis. As per the results shown in the table, among the studied zeolites, chabazite presented the highest relative concentration of aluminum, *i.e.*, 21.8%, and the lowest of silica, *i.e.*, 7.4%. This is habitually considered as a good indicator for an optimal interchange capacity because it leads to a high density of negative charges in the crystalline structure of zeolite that can be replaced by positive cations (Saint-Cricq et al., 2012). In particular, the following Si/Al ratios were observed: 0.34, 6.61, and 2.88 for chabazite, mordenite, and faujasite,

219 respectively. As a result it was determined that the chabazite-type zeolite presented the
220 highest capacity for the metal cation exchange process.

221 Antibacterial and antifungal properties of the unmodified zeolites against different
222 bacteria and fungi are summarized in **Table 3**. In general, all zeolites in their pristine form
223 presented low antimicrobial activity. In relation to the antibacterial tests, carried out by the
224 agar cell counting method, the unmodified zeolites exhibited no biocide activity against *S.*
225 *aureus*. Only the mordenite-type zeolite showed certain reduction, *i.e.*, 60% against *P.*
226 *aeruginosa*. In the case of *E. coli*, interestingly, all zeolites presented certain efficacy, *i.e.*,
227 from 30 to 70% reduction. This indicates that the original cationic nature of the mineral can
228 exert a toxic mechanism within the cell of *E. coli* bacteria. However, the antifungal activity
229 results showed the maximum growth, *i.e.*, 5 in a 0 to 5 scale, for both *A. niger* and *C. albicans*
230 fungi. This means that the traces visible to human eye were greater than 60%.

231

232 ***3.2. Development of metal cation-exchanged zeolites***

233 According to the aforementioned results, chabazite was selected for the ion exchange
234 solution process since this zeolite presented the lowest Si/Al ratio.

235 Samples were observed by SEM to ascertain the effect of the metal cation exchange
236 process on the morphology of the chabazite-type zeolite. SEM micrographs are gathered in
237 **Figure 3**. Particle sizes were kept of in the range of 5–25 μm as shown in **Figures 3a – 3g**.
238 However, remarkably, the presence of coarse particles was reduced in all cases. As compared
239 to the original form shown in previous **Figure 2a**, it can be also observed that more perfect
240 cubic structures emerged during chemical treatment. Therefore, solution treatments by metal
241 cations tended to soften and open up the zeolite surface. As previously indicated, this can be
242 related to the dissolution of amorphous silica fragments of zeolite (Kuronen et al., 2006).
243 Interestingly, the metal cation exchange process did not change the morphology of zeolite
244 crystals. This is consistent with the previous study done by Kwakye-Awuah et al. (Kwakye-
245 Awuah et al., 2008), who incorporated 5.8 wt.-% of silver in faujasite. It was found that
246 zeolites with or without silver showed very similar particle size and appearance, confirming

247 that there was no change in the zeolite structure after the metal cation exchange. A similar
248 effect was observed in the morphology of Ag-zeolite A (Na A) in the research work of
249 Kamisoglu (Kamisoglu et al., 2008).

250 The elemental composition of chabazite after the ion exchange process is given in
251 **Table 4**. Results indicated a good metal cation exchange, which can be detected by the
252 presence of silver, copper, and zinc elements. In particular the silver content in the metal
253 cation-exchanged chabazite-type zeolites was: 1.26% (Reference 1), 1.12% (Reference 4),
254 1.34% (Reference 5), and 1.45% (Reference 7). Therefore, silver loading was similar in all
255 samples, in which the multi-ionic ternary system, *i.e.*, the Ag-Cu-Zn-zeolite, showed the
256 highest value. It is also worthy to mention that lower copper and zinc loadings than silver
257 were attained in chabazite in spite of the higher silver concentration in the solutions. This
258 points out that the ionic exchange process of Ag^{+} on chabazite was more efficient than in the
259 case of Cu^{2+} or Zn^{2+}. The highest content of copper and zinc was again observed for the Ag-
260 Cu-Zn-zeolite, containing 0.293% and 0.116%, respectively.

261 **Table 5** includes a summary of the antimicrobial properties of the metal-cation
262 modified zeolites. According to the table, microorganisms showed different tolerance against
263 these novel engineered zeolites. Among them, Ag-based zeolites (References 1, 4, 5, and 7)
264 presented broader antimicrobial effect than Cu- and Zn-based zeolites (References 2, 3, and
265 6). Modified zeolites without silver, *i.e.*, containing only copper and zinc, partially decreased
266 the number of viable cells of bacteria. However, these systems resulted totally inefficient for
267 fungi, *i.e.*, against *A. niger* and *C. albicans*. Antimicrobial properties of Cu^{2+} were slightly
268 better than Zn^{2+} (References 2 and 4 *vs.* References 3 and 5). *P. aeruginosa* presented higher
269 resistance against Cu^{2+} and Zn^{2+} than *S. aureus* and *E. coli*. The single Ag-zeolite (Reference
270 1) and the ternary Ag-Cu-Zn-zeolite (Reference 7) showed fully antimicrobial activity against
271 all microorganisms. The binary Ag-Cu-zeolite (Reference 4) provided total reduction of
272 microorganisms too. However, the binary Ag-Zn-zeolite (Reference 5) only showed
273 bacteriostatic effect as it partially reduced the growth of *E. coli* and *P. aeruginosa* to 76% and
274 56%, respectively. As previously reported (Kaali et al., 2011), it is possible that in this binary

275 system both cations can block each other and influence their release. The low antibacterial
276 effect observed for single Zn- and Cu-zeolite samples is also in agreement with the recent
277 study performed by Demirci (Demirci et al., 2014). Interestingly, in that study, Cu- and Zn-
278 zeolite samples displayed relatively good antifungal and anticandidal characteristics.

279 The high antimicrobial effect of Ag^{+} in a low-silica zeolite, *i.e.*, chabazite, is in good
280 correlation with previous results in literature. Kwakye-Awuah et al. (Kwakye-Awuah et al.,
281 2008) performed antimicrobial tests for zeolite A and X impregnated with 5.8% of silver.
282 This modified zeolite provided full antimicrobial activity against *S. aureus*, *E. coli*, and *P.*
283 *aeruginosa*. It was particularly found that the modified zeolite released Ag^{+} in a sustained
284 manner to the medium containing the microorganisms. High biocide performance against
285 bacteria and yeast was also reported for Ag-zeolite by Ferreira (Ferreira et al., 2012).
286 Minimum inhibition concentrations (MIC) values in the range of 0.2–0.3 mg/mL were
287 reported. The high antimicrobial activity was related to the presence of metallic silver, *i.e.*,
288 Ag^{0}, on the zeolite pores, in addition to the efficient Ag^{+} release. In a long-term study, MIC
289 values of 32.50 and 61.25 µg/mL were particularly reported for *E. coli* and *S. aureus*,
290 respectively (Bedi et al., 2012). Boschetto et al. (Boschetto et al., 2012) also showed that a
291 concentration of 0.5 mg/mL of Ag-zeolite at 5 wt.-% inhibits bacterial growth.

292 Present results demonstrated that silver-based systems offer superior antimicrobial
293 performance than those based on copper and zinc. However, interestingly, these results also
294 showed the binary Ag-Zn-zeolite (References 4) and ternary binary Ag-Cu-Zn-zeolite
295 (Reference 7) decreased the number of viable cells to a similar extend than the single Ag-
296 zeolite (Reference 1). This implies that the antimicrobial performance of these binary and
297 ternary systems is certainly due to the action of released Ag^{+} ions. However, the biocide
298 effect can be advantageous due to joint activity of Cu^{+2} and Zn^{+2}. This fact is supported by the
299 previously observed efficient incorporation of silver when combined with copper and zinc. In
300 this sense, it was previously indicated that Zn^{+2} could reinforce the antimicrobial activity of
301 Ag^{+} by interfering with cellular proton transfer and inhibiting nutrient uptake (Galeano et al.,
302 2003). Additionally, the presence of Zn element can stabilize the metal exchange framework

303 in zeolite by slowing the release of Ag^+ ions (Cowan et al., 2003). In this sense, it can be
304 assumed that different metal ions initiate different toxic mechanisms in the microorganism
305 cell. Therefore, multi-ionic zeolite systems result more efficient than single ones.

306 Although the precise antimicrobial mechanism of metal-cation exchanged zeolites is
307 certainly complex, it is habitually considered that metal accumulation disrupts bacterial cell
308 walls and other cellular components (Yasuyuki et al., 2010). According to previous studies
309 (Feng et al., 2000; Matsumura et al., 2003), the antimicrobial action of Ag-zeolites occurs in
310 two successive stages. On the one hand, the Ag^+ ions released from porous and voids of
311 zeolite are absorbed on the microorganism cells. This inhibits essential enzymes that are
312 necessary for adenosine triphosphate (ATP) production. Such mechanism can also include
313 plasmolysis and incomplete damage of the cytoplasmic and outer membrane (Yamanaka et
314 al., 2005). On the other hand, reactive oxygen species are generated through the inhibition of
315 respiratory enzymes. These lead to cellular damage and bind with components that interfere
316 with bacterial replication.

317

318 ***3.3. Evaluation of bio-HDPE/metal cation-exchanged zeolites***

319 Due to its highest antibacterial properties, the Ag-Cu-Zn-zeolite (Reference 7) was
320 selected as the filler to functionalize the bio-HDPE matrix. In addition to this, the multi-ionic
321 ternary system presents the advantage to reduce the silver amount in the solution employed
322 for the cation-exchange process.

323 **Figure 4** gathers the tensile properties, *i.e.*, tensile modulus, tensile strength,
324 elongation at break, and Shore D hardness of the unfilled bio-HDPE piece and the pieces
325 filled with Ag-Cu-Zn-zeolite at different loadings. **Figure 4a** illustrates the effect of the filler
326 content on the elastic modulus. An increase in the elasticity of the injection-molded bio-
327 HDPE pieces was observed with the incorporation of Ag-Cu-Zn-zeolite. From 5 wt.-% Ag-
328 Cu-Zn-zeolite, the elastic modulus was doubled, evidencing a stiffening of the bio-HDPE
329 composite pieces. A slight decrease in the tensile strength can be observed in **Figure 4b**. This
330 can be related to a phenomenon of stress concentration by the presence of fillers in the

polymer matrix (Torres-Giner et al., 2016). As shown in **Figure 4c**, addition of Ag-Cu-Zn-zeolite also caused the elongation at break to decrease considerably as compared to that observed for the neat bio-HDPE piece. Some preceding research works related this behavior with the fact that zeolite fillers typically present a porous structure based on small channels. Polymer chains could then penetrate into the cavities of the inorganic structure, which restricts chain mobility (Biswas et al., 2003; Biswas et al., 2004). Other factors, such as a zeolite particle size and shape, can also influence (Ciobanu et al., 2007). In relation to the D hardness, the presence of Ag-Cu-Zn-zeolite led to a significant increase. As reflected in **Figure 4d**, for injection-molded bio-HDPE composite pieces containing Ag-Cu-Zn-zeolite at 15 wt.-%, Shore D hardness was *ca.* 17% higher than that of the unfilled bio-HDPE piece.

The enhancement of the mechanical resistance against elastic deformation upon the incorporation of zeolites in bio-HDPE can be regarded as a positive aspect for rigid applications. The above-mentioned results are also in agreement with some previous studies for other polymer matrices. For instance, a similar mechanical increase was observed for TPU/zeolite composites (Kamisoglu et al., 2008). Zampino et al. (Zampino et al., 2011) also reported a monotonic increase of the elastic modulus of PVC as the amount of Ag-zeolite was increased in the polymer composite. Similarly, Li et al. (Li et al., 2013) observed that the addition of zinc oxide (ZnO)-modified zeolites slightly increased the flexural modulus and tensile strength of PP random copolymer. That study also showed that the modified zeolites decreased the flexural strength, elongation at break, and impact strength. In another recent study, Mishra et al. (Mishra et al., 2013) interestingly showed that the addition of up to 20 wt.-% of clinoptilolite-type zeolite treated with hydrochloric acid (HCl) increased the Young's modulus of EVA from 420.7 to 537.6 MPa. It was reported that higher contents led to certain agglomeration, which impaired the films brittleness. A decrease in the mechanical properties of PP/zeolites composites was also reported by Pehlivan et al. (Pehlivan et al., 2005). The mechanical weakening was explained by the formation of voids around the fillers due to poor bonding between the zeolite particles and the PP matrix.

As it can be seen in **Table 6**, the unfilled bio-HDPE piece showed no inhibition effect on bacterial growth. Alternatively, all injection-molded composite pieces exhibited significant antibacterial activity against *S. aureus, E. coli*, and *P. aeruginosa*. In particular, the addition of Ag-Cu-Zn-zeolite in the range of 1-5 wt.-% led to a remarkable increase in antibacterial response with R values close to 2.5-3.0 (bacteriostatic effect) for *S. aureus* and higher than 4 for *E. coli* and *P. aeruginosa* (bactericidal effect). The optimal content was then observed for the bio-HDPE/Ag-Cu-Zn-zeolite piece at 1 wt.-% because this composite is representative for a high antibacterial activity with the lowest filler loading. Higher Ag-Cu-Zn-zeolite loadings, *i.e.*, 10 and 15 wt.-%, resulted in a full antibacterial performance.

Accomplished antibacterial performance is in relatively good agreement with preceding results for other polymer composites. However, the attained results are difficult to compare with those found in the literature because the antimicrobial activity exerted by zeolites can be influenced by many different parameters. Indeed, the biocide effect mainly depends on the release mechanism of the metal cations that are tightly bonded to the zeolite structure. This can be further related to the polymer matrix, zeolite content, method to obtain the composites, antimicrobial test, ionic strength of medium, etc. As an example, Zampino et al. (Zampino et al., 2011) showed high antimicrobial activity of PVC/Ag-zeolites composites against both *E. coli* and *S. epidermidis* after 24h in a medium of TSB. A significant reduction (10^3 CFU/mL) was observed in the composite when compared to the neat PVC (10^9 CFU/mL). In relation to bioplastic matrices, Fernandez et al. (Fernandez et al., 2010) showed that PLA/Ag-zeolite films at 5 wt.-%, obtained by solution casting, were able to decrease by *ca.* 90% the growth of *E. coli* and *S. aureus* after 24h in aqueous solution. Interestingly, the antimicrobial activity of thermoformed films containing equivalent amounts of Ag-zeolite was negligible. A similar effect was observed by Boschetto (Boschetto et al., 2012) for LDPE, in which composite films containing 5 wt.-% Ag-zeolite obtained by wet casting performed considerably better against *E. coli* than corresponding hot-pressed films. According to the authors, this effect occurred due to the high temperatures employed during

385 the composites preparation that could affect the stability of silver. These previous
386 observations reinforce the novelty of the achieved results in the present study.
387
388 **Conclusions**
389 Novel sustainable composite pieces were prepared by the incorporation of
390 antimicrobial metal cation-exchanged zeolites into bio-HDPE. This method involved the prior
391 selection and functionalization of pristine zeolites by Ag^{+}, Cu^{+2}, and Zn^{+2}. The chabazite–type
392 zeolite was chosen due to its improved morphology and lowest Si/Al. Optimal antimicrobial
393 results were observed for the ternary Ag-Cu-Zn-zeolite since it provide full antimicrobial
394 performance and reduced the amount of added silver. This was then melt processed in a twin-
395 screw extruder in powder form with the biopolymer and shaped by injection molding.
396 Obtained injection-molded composite pieces resulted in superior elastic modulus and
397 hardness as compared to the unfilled bio-HDPE piece. Mechanical results indicated that the
398 injection-molded metal-loaded zeolite composite pieces are potential candidates for rigid
399 applications. Antibacterial results on the test surface confirmed good perspectives for the
400 novel composite pieces with Ag-Cu-Zn-zeolite contents as low as 1 wt.-%. These sustainable
401 cost-effective composites can be of relevant interest to control the growth of harmful
402 microorganisms in environments for processing, preparation, and storage of food.
403
404 **Acknowledgements**
405 This research was supported by the Spanish Ministry of Economy and Competitiveness
406 (Project MAT2014-59242-C2-1-R). The authors also thank “Conselleria d'Educació, Cultura i
407 Esport – Generalitat Valenciana” (grant number GV/2014/008) for financial support.
408
409 **References**
410 APPENDINI, P. and HOTCHKISS, J.H. 2002. Review of antimicrobial food packaging.
411 Innovative Food Science and Emerging Technologies. 3**,** 113-126.
412 BABU, R.P., O'CONNOR, K. and RAMAKRISHNA, S. 2013. Current progress on bio-based
413 polymers and their future trends. Progress in Biomaterials. 2**,** 1-16.

BEDI, R.S., CAI, R., O'NEILL, C., BEVING, D.E., FOSTER, S., GUTHRIE, S., CHEN, W. and YAN, Y. 2012. Hydrophilic and antimicrobial Ag-exchanged zeolite a coatings: A year-long durability study and preliminary evidence for their general microbiocidal efficacy to bacteria, fungus and yeast. Microporous and Mesoporous Materials. 151**,** 352-357.

BISWAS, J., KIM, H., CHOE, S.J., KUNDU, P.P., PARK, Y.H. and LEE, D.S. 2003. Linear low density polyethylene (LLDPE)/zeolite microporous composite film. Macromolecular Research. 11**,** 357-367.

BISWAS, J., KIM, H., YIM, C.S., CHO, J., KIM, G.J., CHOE, S. and LEE, D.S. 2004. Structural effects on the tensile and morphological properties of zeolite-filled polypropylene derivative composites. Macromolecular Research. 12**,** 443-450.

BOSCHETTO, D.L., LERIN, L., CANSIAN, R., PERGHER, S.B.C. and DI LUCCIO, M. 2012. Preparation and antimicrobial activity of polyethylene composite films with silver exchanged zeolite-Y. Chemical Engineering Journal. 204**,** 210-216.

CHEN, G., LI, S., JIAO, F. and YUAN, Q. 2007. Catalytic dehydration of bioethanol to ethylene over TiO2/gamma-Al2O3 catalysts in microchannel reactors. Catalysis Today. 125**,** 111-119.

CIOBANU, G., CARJA, G. and CIOBANU, O. 2007. Preparation and characterization of polymer-zeolite nanocomposite membranes. Materials Science & Engineering C-Biomimetic and Supramolecular Systems. 27**,** 1138-1140.

CORMA, A. and GARCIA, H. 2004. Supramolecular host-guest systems in zeolites prepared by ship-in-a-bottle synthesis. European Journal of Inorganic Chemistry. 2004**,** 1143-1164.

COWAN, M.M., ABSHIRE, K.Z., HOUK, S.L. and EVANS, S.M. 2003. Antimicrobial efficacy of a silver-zeolite matrix coating on stainless steel. Journal of Industrial Microbiology & Biotechnology. 30**,** 102-106.

CZARAN, E., PAPP, J., MESZAROSKIS, A. and DOMOKOS, E. 1989. Ag-ion exchange by natural mordenite and clinoptilolite. Acta Chimica Hungarica-Models in Chemistry. 126**,** 673-683.

DEL NOBILE, M.A., CANNARSI, M., ALTIERI, C., SINIGAGLIA, M., FAVIA, P., IACOVIELLO, G. and D'AGOSTINO, R. 2004. Effect of Ag-containing nano-composite active packaging system on survival of Alicyclobacillus acidoterrestris. Journal of Food Science. 69**,** E379-E383.

DEMIRCI, S., USTAOGLU, Z., YILMAZER, G.A., SAHIN, F. and BAC, N. 2014. Antimicrobial Properties of Zeolite-X and Zeolite-A Ion-Exchanged with Silver, Copper, and Zinc Against a Broad Range of Microorganisms. Applied Biochemistry and Biotechnology. 172**,** 1652-1662.

DUNCAN, T.V. 2011. Applications of nanotechnology in food packaging and food safety: Barrier materials, antimicrobials and sensors. Journal of Colloid and Interface Science. 363**,** 1-24.

EGGER, S., LEHMANN, R.P., HEIGHT, M.J., LOESSNER, M.J. and SCHUPPLER, M. 2009. Antimicrobial Properties of a Novel Silver-Silica Nanocomposite Material. Applied and Environmental Microbiology. 75**,** 2973-2976.

FENG, Q.L., WU, J., CHEN, G.Q., CUI, F.Z., KIM, T.N. and KIM, J.O. 2000. A mechanistic study of the antibacterial effect of silver ions on Escherichia coli and Staphylococcus aureus. Journal of Biomedical Materials Research. 52**,** 662-668.

FERNANDEZ, A., SORIANO, E., HERNANDEZ-MUNOZ, P. and GAVARA, R. 2010. Migration of Antimicrobial Silver from Composites of Polylactide with Silver Zeolites. Journal of Food Science. 75**,** E186-E193.

FERREIRA, L., FONSECA, A.M., BOTELHO, G., ALMEIDA-AGUIAR, C. and NEVES, I.C. 2012. Antimicrobial activity of faujasite zeolites doped with silver. Microporous and Mesoporous Materials. 160**,** 126-132.

GALEANO, B., KORFF, E. and NICHOLSON, W.L. 2003. Inactivation of vegetative cells, but not spores, of Bacillus anthracis, B-cereus, and B-subtilis on stainless steel surfaces coated with an antimicrobial silver- and zinc-containing zeolite formulation. Applied and Environmental Microbiology. 69**,** 4329-4331.

GEHRKE, I., GEISER, A. and SOMBORN-SCHULZ, A. 2015. Innovations in nanotechnology for water treatment. Nanotechnology, science and applications. 8**,** 1-17.

GRIFFITH, A., NEETHIRAJAN, S. and WARRINER, K. 2015. Development and Evaluation of Silver Zeolite Antifouling Coatings on Stainless Steel for Food Contact Surfaces. Journal of Food Safety. 35**,** 345-354.

INOUE, Y. and HAMASHIMA, H. 2012. Effect of silver-loaded zeolite on the susceptibility of Escherichia coli against antibiotics. Journal of Biomaterials and Nanobiotechnology. 3**,** 114-117.

KAALI, P., PEREZ-MADRIGAL, M.M., STROMBERG, E., AUNE, R.E., CZEL, G. and KARLSSON, S. 2011. The influence of Ag+, Zn2+ and Cu2+ exchanged zeolite on antimicrobial and long term in vitro stability of medical grade polyether polyurethane. Express Polymer Letters. 5**,** 1028-1040.

KAMISOGLU, K., AKSOY, E.A., AKATA, B., HASIRCI, N. and BAC, N. 2008. Preparation and Characterization of Antibacterial Zeolite-Polyurethane Composites. Journal of Applied Polymer Science. 110**,** 2854-2861.

KRISHNANI, K.K., ZHANG, Y., XIONG, L., YAN, Y., BOOPATHY, R. and MULCHANDANI, A. 2012. Bactericidal and ammonia removal activity of silver ion-exchanged zeolite. Bioresource Technology. 117**,** 86-91.

KURONEN, M., WELLER, M., TOWNSEND, R. and HARJULA, R. 2006. Ion exchange selectivity and structural changes in highly aluminous zeolites. Reactive & Functional Polymers. 66**,** 1350-1361.

KWAKYE-AWUAH, B., WILLIAMS, C., KENWARD, M.A. and RADECKA, I. 2008. Antimicrobial action and efficiency of silver-loaded zeolite X. Journal of Applied Microbiology. 104**,** 1516-1524.

LALUEZA, P., CARMONA, D., MONZON, M., ARRUEBO, M. and SANTAMARIA, J. 2012. Strong bactericidal synergy between peracetic acid and silver-exchanged zeolites. Microporous and Mesoporous Materials. 156**,** 171-175.

LI, M., LI, G., JIANG, J., TAO, Y. and MAI, K.C. 2013. Preparation, antimicrobial, crystallization and mechanical properties of nano-ZnO-supported zeolite filled polypropylene random copolymer composites. Composites Science and Technology. 81**,** 30-36.

LOPES, A.C., CAPARROS, C., FERDOV, S. and LANCEROS-MENDEZ, S. 2013. Influence of zeolite structure and chemistry on the electrical response and crystallization phase of poly(vinylidene fluoride). Journal of Materials Science. 48**,** 2199-2206.

MATSUMURA, Y., YOSHIKATA, K., KUNISAKI, S. and TSUCHIDO, T. 2003. Mode of bactericidal action of silver zeolite and its comparison with that of silver nitrate. Applied and Environmental Microbiology. 69**,** 4278-4281.

MISHRA, A.K., MISHRA, S.B., MAMBA, B.B., DLAMINI, D.S. and MTHOMBO, T.S. 2013. Fabrication and characterization of HCl-treated clinoptilolite filled ethylene vinyl acetate composite films. Journal of Applied Polymer Science. 127**,** 4359-4365.

MØRETRØ, T., HOIBY-PETTERSEN, G.S., HALVORSEN, C.K. and LANGSRUD, S. 2012. Antibacterial activity of cutting boards containing silver. Food Control. 28**,** 118-121.

MØRETRØ, T. and LANGSRUD, S. 2011. Effects of Materials Containing Antimicrobial Compounds on Food Hygiene. Journal of Food Protection. 74**,** 1200-1211.

NARIN, G., ALBAYRAK, C.B. and ULKU, S. 2014. Preparation and characterization of antibacterial cobalt-exchanged natural zeolite/poly(vinyl alcohol) hydrogels. Journal of Sol-Gel Science and Technology. 69**,** 214-230.

PEHLIVAN, H., BALKOSE, D., ULKU, S. and TIHMINLIOGLU, F. 2005. Characterization of pure and silver exchanged natural zeolite filled polypropylene composite films. Composites Science and Technology. 65**,** 2049-2058.

RAI, M., YADAV, A. and GADE, A. 2009. Silver nanoparticles as a new generation of antimicrobials. Biotechnology Advances. 27**,** 76-83.

REIJ, M.W., DEN AANTREKKER, E.D. and MICROBIO, I.E.R.A. 2004. Recontamination as a source of pathogens in processed foods. International Journal of Food Microbiology. 91**,** 1-11.

ROZIC, M., CERJAN-STEFANOVIC, S., KURAJICA, S., VANCINA, V. and HODZIC, E. 2000. Ammoniacal nitrogen removal from water by treatment with clays and zeolites. Water Research. 34**,** 3675-3681.

SAINT-CRICQ, P., KAMIMURA, Y., ITABASHI, K., SUGAWARA-NARUTAKI, A., SHIMOJIMA, A. and OKUBO, T. 2012. Antibacterial Activity of Silver-Loaded "Green Zeolites". European Journal of Inorganic Chemistry. 3398-3402.

SUIB, S.L. 2003. Handbook of zeolite science and technology. Science. 302**,** 1335-1336.

TOP, A. and ULKU, S. 2004. Silver, zinc, and copper exchange in a Na-clinoptilolite and resulting effect on antibacterial activity. Applied Clay Science. 27**,** 13-19.

TORRES-GINER, S. 2011. *Novel Antimicrobials Obtained by Electrospinning Methods, in Antimicrobial Polymers (eds J.M. Lagaron, M.J. Ocio and A. Lopez-Rubio)*. John Wiley & Sons, Inc., Hoboken, NJ, USA.

TORRES-GINER, S., MARTINEZ-ABAD, A. and LAGARON, J.M. 2014. Zein-based ultrathin fibers containing ceramic nanofillers obtained by electrospinning. II. Mechanical properties, gas barrier, and sustained release capacity of biocide thymol in multilayer polylactide films. Journal of Applied Polymer Science. 131**,** 9270-9276.

TORRES-GINER, S., MONTANES, N., FENOLLAR, O., GARCÍA-SANOGUERA, D. and BALART, R. 2016. Development and optimization of renewable vinyl plastisol/wood flour composites exposed to ultraviolet radiation. Materials & Design. 108**,** 648-658.

YAMANAKA, M., HARA, K. and KUDO, J. 2005. Bactericidal actions of a silver ion solution on Escherichia coli, studied by energy-filtering transmission electron microscopy and proteomic analysis. Applied and Environmental Microbiology. 71**,** 7589-7593.

YANG, W., SHEN, C., JI, Q., AN, H., WANG, J., LIU, Q. and ZHANG, Z. 2009. Food storage material silver nanoparticles interfere with DNA replication fidelity and bind with DNA. Nanotechnology. 20**,** 085102.

YASUYUKI, M., KUNIHIRO, K., KURISSERY, S., KANAVILLIL, N., SATO, Y. and KIKUCHI, Y. 2010. Antibacterial properties of nine pure metals: a laboratory study using Staphylococcus aureus and Escherichia coli. Biofouling. 26**,** 851-858.

ZAMPINO, D., FERRERI, T., PUGLISI, C., MANCUSO, M., ZACCONE, R., SCAFFARO, R. and BENNARDO, D. 2011. PVC silver zeolite composites with antimicrobial properties. Journal of Materials Science. 46**,** 6734-6743.

Table Captions

Table 1. Summary of the metal cation exchange solutions based on silver nitrate $(AgNO)_3$, copper nitrate $(Cu(NO_3)_2)$, and zinc nitrate $(Zn(NO_3)_2)$. References were described according to the presence of silver (Ag^+), copper (Cu^{2+}), and zinc (Zn^{2+}) ions.

Table 2. Elemental composition of the unmodified zeolites obtained by X-ray fluorescence (XRF).

Table 3. Antimicrobials properties of the unmodified zeolites against *Staphylococcus aureus (S. aureus)*, *Escherichia coli (E. coli)*, *Pseudomonas aeruginosa (P. aeruginosa)*, *Aspergilus niger* (*A. niger*), and *Candida albicans* (*C. albicans*). Antibacterial results were expressed as the percentage decrease in the colony forming units per milliliter (CFU/mL). Antifungal properties were expressed as the visual growth range.

Table 4. Elemental composition of the metal cation-exchanged chabazite-type zeolite by X-ray fluorescence (XRF).

Table 5. Antimicrobials properties of the metal cation-exchanged chabazite-type zeolites against *Staphylococcus aureus (S. aureus)*, *Escherichia coli (E. coli)*, *Pseudomonas aeruginosa (P. aeruginosa)*, *Aspergilus niger* (*A. niger*), and *Candida albicans* (*C. albicans*). Antibacterial results were expressed as the percentage reduction in the colony forming units per milliliter (CFU/mL). Antifungal properties were expressed as the visual growth range. Biocide effect was described according to the presence of silver (Ag^+), copper (Cu^{2+}), and zinc (Zn^{2+}) ions.

Table 6. Antibacterial properties of the injection-molded composite pieces as a function of the weight content (wt.-%) of the metal cation-exchanged chabazite-type zeolite against *Staphylococcus aureus (S. aureus)*, *Escherichia coli (E. coli)*, and *Pseudomonas aeruginosa (P. aeruginosa)*. Results were expressed as the test surface reduction (R).

589 **Figure Captions**

590

591 **Figure 1**. Schematic representation of the metal cation exchange process performed on
592 zeolite.

593 **Figure 2**. Scanning electron microscopy (SEM) images at different magnifications of: a)
594 Chabazite; b) Mordenite; c) Faujasite. Scale markers of 100, 60, and 30 μm in all cases.

595 **Figure 3**. Scanning electron microscopy (SEM) images at different magnifications of the
596 chabazite-type zeolite exchanged with silver (Ag^{+}), copper (Cu^{+2}), and zinc (Zn^{+2}) ions: a)
597 Ag-zeolite (Reference 1); b) Cu-zeolite (Reference 2); c) Zn-zeolite (Reference 3); d) Ag-Cu-
598 zeolite (Reference 4); e) Ag-Zn-zeolite (Reference 5); f) Cu-Zn-zeolite (Reference 6); g) Ag-
599 Cu-Zn-zeolite (Reference 7). Scale markers of 100, 60, and 30 μm in all cases.

600 **Figure 4**. Mechanical properties of the injection-molded pieces of bio-based high-density
601 polyethylene (bio-HDPE) as a function of the weight content (wt.-%) of Ag-Cu-Zn-zeolite: a)
602 Tensile modulus; b) Tensile strength; c) Elongation at break; d) Shore D hardness. The
603 chabazite-type zeolite was exchanged with silver (Ag^{+}), copper (Cu^{+2}), and zinc (Zn^{+2}) ions.

Table 1. Summary of the metal cation exchange solutions based on silver nitrate $(AgNO)_3$, copper nitrate $(Cu(NO_3)_2)$, and zinc nitrate $(Zn(NO_3)_2)$. References were described according to the presence of silver (Ag^+), copper (Cu^{2+}), and zinc (Zn^{2+}) ions.

Description		**Solution (mL)**		
Reference	**Metal cation**	**0.07M $AgNO_3$**	**0.4M $Cu(NO_3)_2 \cdot 3H2O$**	**0.2M $Zn(NO_3)_2 \cdot 6H2O$**
1	Ag^+	150		
2	Cu^{2+}		150	
3	Zn^{2+}			150
4	$Ag^+ + Cu^{2+}$	75	75	
5	$Ag^+ + Zn^{2+}$	75		75
6	$Cu^{2+} + Zn^{2+}$		75	75
7	$Ag^+ + Cu^{2+} + Zn^{2+}$	50	50	50

Table 2. Elemental composition of the unmodified zeolites obtained by X-ray fluorescence (XRF).

Element	Relative content (%)		
	Chabazite	**Mordenite**	**Faujasite**
Oxygen (O)	52.000 ± 2.150	50.600 ± 3.620	48.200 ± 2.550
Aluminum (Al)	21.800 ± 1.260	5.7500 ± 0.350	10.700 ± 0.750
Phosphorus (P)	18.800 ± 1.010	0.142 ± 0.001	0.002 ± 0.001
Silicon (Si)	7.400 ± 0.370	38.000 ± 1.780	30.800 ± 1.190
Sodium (Na)	< 0.001	5.160 ± 1.250	10.200 ± 0.650
Titanium (Ti)	< 0.001	0.250 ± 0.005	< 0.001
Iron (Fe)	0.016 ± 0.001	0.080 ± 0.001	0.002 ± 0.001
Potassium (K)	< 0.001	0.045 ± 0.025	0.038 ± 0.001
Barium (Ba)	< 0.001	0.017 ± 0.001	< 0.001
Calcium (Ca)	0.009 ± 0.001	0.008 ± 0.001	0.008 ± 0.001
Gallium (Ga)	0.006 ± 0.001	< 0.001	< 0.001
Strontium (Sr)	< 0.001	0.005 ± 0.001	< 0.001
Zirconium (Zr)	< 0.001	0.005 ± 0.001	0.002 ± 0.001

Table 3. Antimicrobials properties of the unmodified zeolites against *Staphylococcus aureus (S. aureus)*, *Escherichia coli (E. coli)*, *Pseudomonas aeruginosa (P. aeruginosa)*, *Aspergilus niger* (*A. niger*), and *Candida albicans* (*C. albicans*). Antibacterial results were expressed as the percentage decrease in the colony forming units per milliliter (CFU/mL). Antifungal properties were expressed as the visual growth range.

Zeolites	**% Reduction (UFC/mL)**			**Growth range**	
	S. aureus	***E. coli***	***P. aeruginosa***	***A. niger***	***C. albicans***
Chabazite	0	70.0 ± 5.1	0	5	5
Mordenite	0	52.0 ± 2.3	60.0 ± 4.0	5	5
Faujasite	0	29.0 ± 1.8	0	5	5

Table 4. Elemental composition of the metal cation-exchanged chabazite-type zeolite by X-ray fluorescence (XRF).

Element	Relative content (%)						
	Reference 1	**Reference 2**	**Reference 3**	**Reference 4**	**Reference 5**	**Reference 6**	**Reference 7**
Oxygen (O)	51.400 ± 3.500	52.000 ± 2.800	51.800 ± 3.310	51.500 ± 2.925	51.400 ± 3.690	52.000 ± 1.900	51.200 ± 3.450
Aluminum (Al)	21.600 ± 2.450	21.400 ± 1.900	21.100 ± 1.120	20.500 ± 0.850	21.000 ± 1.750	21.200 ± 1.240	21.000 ± 2.050
Phosphorus (P)	18.500 ± 1.760	19.000 ± 1.670	18.700 ± 0.900	19.100 ± 1.375	18.800 ± 0.650	19.000 ± 0.540	18.800 ± 0.100
Silicon (Si)	7.230 ± 0.440	7.320 ± 0.560	7.540 ± 0.050	7.390 ± 0.001	7.360 ± 0.375	7.430 ± 0.080	7.110 ± 0.060
Silver (Ag)	1.260 ± 0.009	< 0.001	< 0.001	1.120 ± 0.001	1.340 ± 0.008	< 0.001	1.450 ± 0.015
Copper (Cu)	< 0.001	0.179 ± 0.001	< 0.001	0.283 ± 0.001	< 0.001	0.284 ± 0.003	0.293 ± 0.009
Zinc (Zn)	< 0.001	< 0.001	0.135 ± 0.010	< 0.001	0.097 ± 0.005	0.087 ± 0.002	0.116 ± 0.007
Iron (Fe)	0.011 ± 0.001	0.016 ± 0.002	< 0.001	< 0.001	0.014 ± 0.001	< 0.001	< 0.001
Calcium (Ca)	0.089 ± 0.001	0.010 ± 0.001	0.009 ± 0.001	0.010 ± 0.001	0.010 ± 0.001	0.010 ± 0.001	0.010 ± 0.001
Gallium (Ga)	0.007 ± 0.001	0.006 ± 0.001	0.005 ± 0.001	0.008 ± 0.001	0.010 ± 0.001	0.007 ± 0.001	0.009 ± 0.001
Potassium (K)	< 0.001	0.021 ± 0.004	< 0.001	< 0.001	< 0.001	< 0.001	< 0.001
Sodium (Na)	< 0.001	< 0.001	0.673 ± 0.003	< 0.001	< 0.001	< 0.001	< 0.001

Table 5. Antimicrobials properties of the metal cation-exchanged chabazite-type zeolites against *Staphylococcus aureus (S. aureus)*, *Escherichia coli (E. coli)*, *Pseudomonas aeruginosa (P. aeruginosa)*, *Aspergilus niger* (*A. niger*), and *Candida albicans* (*C. albicans*). Antibacterial results were expressed as the percentage reduction in the colony forming units per milliliter (CFU/mL). Antifungal properties were expressed as the visual growth range. Biocide effect was described according to the presence of silver (Ag^{+}), copper (Cu^{2+}), and zinc (Zn^{2+}) ions.

Description		**% Reduction (UFC/mL)**			**Growth range**	
Reference	**Metal cation**	***S. aureus***	***E. coli***	***P. aeruginosa***	***A. niger***	***C. albicans***
1	**Ag^{+}**	99.9 ± 0.2	99.9 ± 0.1	99.9 ± 0.1	0	0
2	**Cu^{2+}**	48.0 ± 1.8	75.0 ± 2.8	30.0 ± 1.9	5	5
3	**Zn^{2+}**	69.0 ± 1.4	57.0 ± 3.5	3.0 ± 0.6	5	5
4	**Ag^{+} + Cu^{2+}**	99.4 ± 0.2	99.6 ± 0.1	99.9 ± 0.1	0	0
5	**Ag^{+} + Zn^{2+}**	99.7 ± 0.3	76.0 ± 1.2	56.0 ± 2.7	0	0
6	**Cu^{2+} + Zn^{2+}**	58.0 ± 3.8	99.9 ± 0.1	59.0 ± 4.2	5	5
7	**Ag^{+} + Cu^{2+} + Zn^{2+}**	99.9 ± 0.1	99.8 ± 0.1	99.9 ± 0.1	0	0

Table 6. Antibacterial properties of the injection-molded composite pieces as a function of the weight content (wt.-%) of the metal cation-exchanged chabazite-type zeolite against *Staphylococcus aureus (S. aureus)*, *Escherichia coli (E. coli)*, and *Pseudomonas aeruginosa (P. aeruginosa)*. Results were expressed as the test surface reduction (R).

Zeolite content (wt.-%)	**R value**		
	S. aureus	***E. coli***	***P. aeruginosa***
0	0.02 ± 0.01	0.7 ± 0.01	0.53 ± 0.02
1	2.24 ± 0.20	4.11 ± 0.02	4.10 ± 0.01
5	2.77 ± 0.30	4.11 ± 0.01	4.10 ± 0.03
10	3.96 ± 0.05	4.11 ± 0.02	4.10 ± 0.03
15	3.96 ± 0.05	4.11 ± 0.03	4.10 ± 0.02

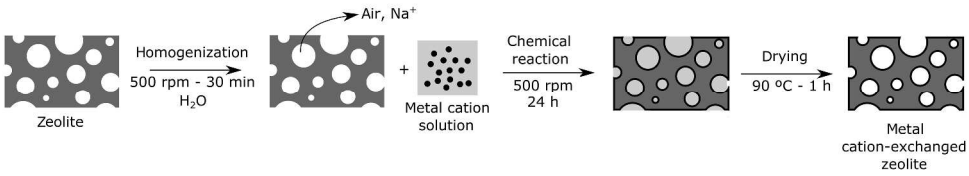

Figure 1. Schematic representation of the metal cation exchange process performed on zeolite.
Figue1
338x70mm (300 x 300 DPI)

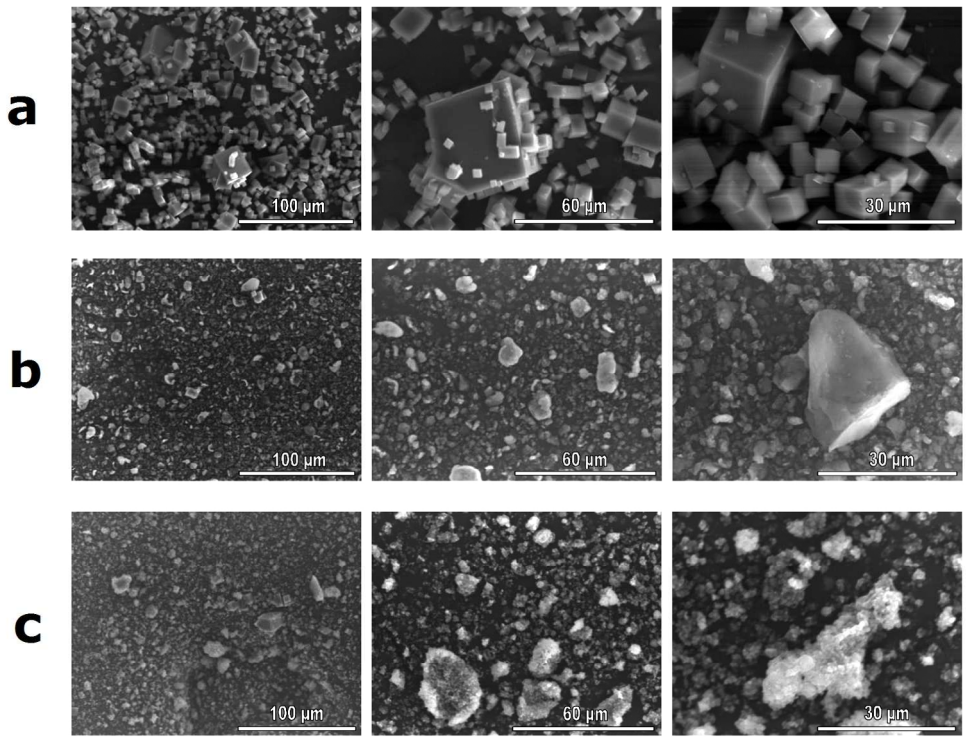

Figure 2. Scanning electron microscopy (SEM) images at different magnifications of: a) Chabazite; b) Mordenite; c) Faujasite. Scale markers of 100, 60, and 30 µm in all cases.
Figure 2
172x133mm (300 x 300 DPI)

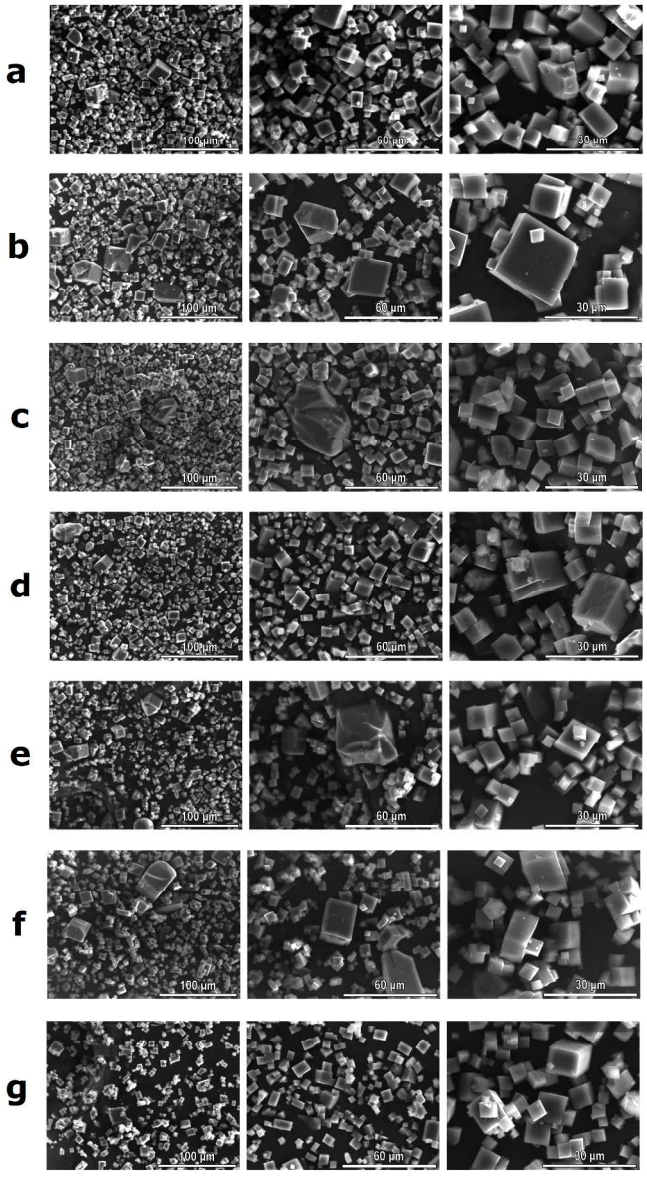

Figure 3. Scanning electron microscopy (SEM) images at different magnifications of the chabazite-type zeolite exchanged with silver (Ag+), copper (Cu+2), and zinc (Zn+2) ions: a) Ag-zeolite (Reference 1); b) Cu-zeolite (Reference 2); c) Zn-zeolite (Reference 3); d) Ag-Cu-zeolite (Reference 4); e) Ag-Zn-zeolite (Reference 5); f) Cu-Zn-zeolite (Reference 6); g) Ag-Cu-Zn-zeolite (Reference 7). Scale markers of 100, 60, and 30 µm in all cases.

Figure 3

172x310mm (300 x 300 DPI)

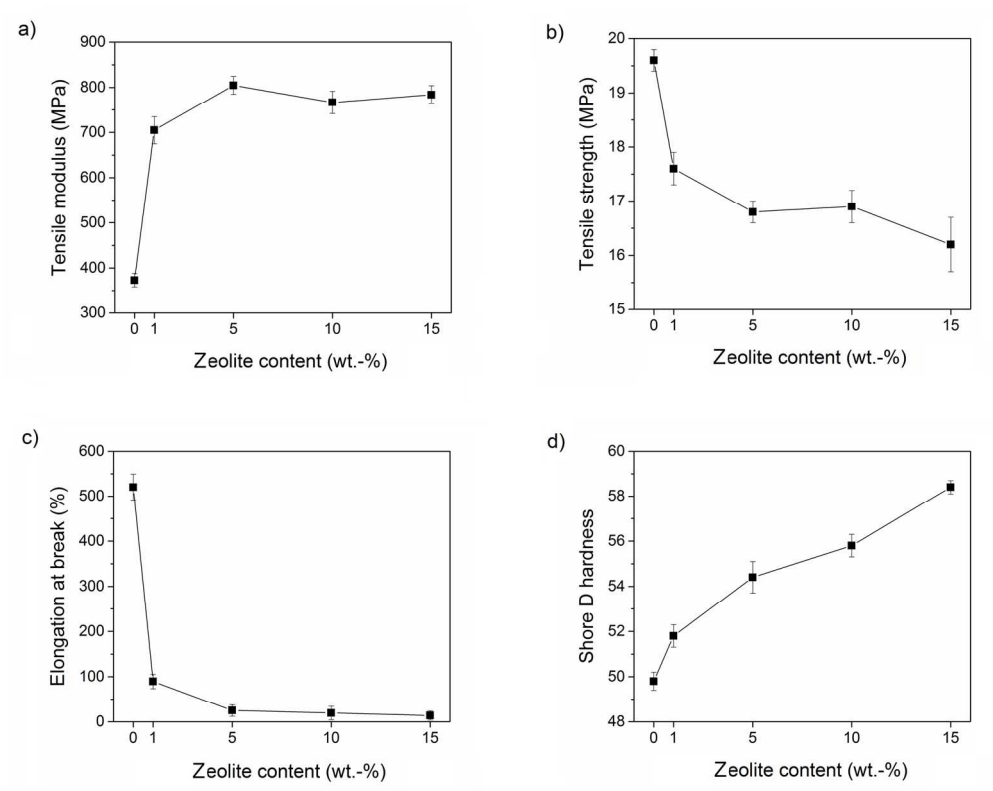

Figure 4. Mechanical properties of the injection-molded pieces of bio-based high-density polyethylene (bio-HDPE) as a function of the weight content (wt.-%) of Ag-Cu-Zn-zeolite: a) Tensile modulus; b) Tensile strength; c) Elongation at break; d) Shore D hardness. The chabazite-type zeolite was exchanged with silver (Ag+), copper (Cu2+), and zinc (Zn2+) ions.

Figure 4

169x134mm (300 x 300 DPI)